

A SUPERNOVA ORIGIN FOR DUST IN A HIGH-REDSHIFT QUASAR

R. Maiolino ^{*}, R. Schneider ^{†*}, E. Oliva ^{‡*}, S. Bianchi [§],
 A. Ferrara [¶], F. Mannucci[§], M. Pedani[‡], M. Roca Sogorb ^{||}

^{*} INAF - Osservatorio Astrofisico di Arcetri, Largo Enrico Fermi 5, 50125 Firenze, Italy

[†] “Enrico Fermi” Center, Via Panisperna 89/A, 00184 Roma, Italy

[‡] Telescopio Nazionale Galileo, C. Alvarez de Abreu, 70, 38700 S.ta Cruz de La Palma, Spain

[§] CNR-IRA, Sezione di Firenze, Largo Enrico Fermi 5, 50125 Firenze, Italy

[¶] SISSA/International School for Advanced Studies, Via Beirut 4, 34100 Trieste, Italy

^{||} Astrofisico Fco. Sánchez, Universidad de La Laguna, 38206 La Laguna, Tenerife, Spain

Interstellar dust plays a crucial role in the evolution of the Universe by assisting the formation of molecules¹, by triggering the formation of the first low-mass stars², and by absorbing stellar ultraviolet-optical light and subsequently re-emitting it at infrared/millimetre wavelengths. Dust is thought to be produced predominantly in the envelopes of evolved (age >1 Gyr), low-mass stars³. This picture has, however, recently been brought into question by the discovery of large masses of dust in the host galaxies of quasars^{4,5} at redshift $z > 6$, when the age of the Universe was less than 1 Gyr. Theoretical studies^{6,7,8}, corroborated by observations of nearby supernova remnants^{9,10,11}, have suggested that supernovae provide a fast and efficient dust formation environment in the early Universe. Here we report infrared observations of a quasar at redshift 6.2, which are used to obtain directly its dust extinction curve. We then show that such a curve is in excellent agreement with supernova dust models. This result demonstrates a supernova origin for dust in this high-redshift quasar, from which we infer that most of the dust at high redshifts has probably the same origin.

Powerful quasars offer an optimal tool for detailed studies of dust in their host galaxies out to very high redshifts. Dust extinction is inferred through reddening of the quasar UV/optical continuum emission. The extinction curve ($A_\lambda = 1.086 \tau_\lambda$, where τ_λ is the wavelength-dependent optical depth) of dust associated with low redshift, mildly obscured quasars has been typically found to be consistent with that of the Small Magellanic Cloud (SMC)^{12,13,14}, while for heavily absorbed quasars there are indications that the extinction curve may be different^{15,16}.

An important class of quasars are the Broad Absorption Line (BAL) quasars, whose UV spectrum is characterized by blueshifted, deep and broad absorption features associated with highly ionized atomic species, which trace powerful outflows of dense gas along our line of sight. Low Ionization BAL (LoBAL) quasars are characterized by additional low ionization absorption lines, probably associated with higher column densities of gas. LoBAL quasars at $z < 4$ are *always* significantly reddened by dust (associated with the outflowing gas), and therefore they are ideal

laboratories to investigate the properties of dust.

By means of low resolution near-IR spectroscopic observations we have recently identified a few BAL quasars at $z \approx 5 - 6$ (Maiolino et al. 2004). The most distant among them is the LoBAL quasar SDSSJ104845.05+463718.3 (hereafter SDSS1048+46). At a redshift $z = 6.193$ (based on a new medium resolution spectrum around $\text{MgII}\lambda 2798$; Maiolino et al. in prep), this is the only LoBAL at $z > 5$ currently known, and offers a unique chance of investigating the dust extinction curve at $z \approx 6$. This quasar was re-observed at higher spectral resolution with the goal of de-blending the deep troughs characterizing its spectrum and of estimating the reddening of the continuum. Observations were obtained in February 2004 with the Near Infrared Camera Spectrometer (NICS¹⁸) at the Telescopio Nazionale Galileo (Canary Islands). SDSS1048+46 was observed for a total of 3 hours, with a slit of $1.5''$ oriented along the parallactic angle. We used a grism covering the spectral region $0.8 - 1.45\mu\text{m}$.

Fig. 1a shows the observed spectrum (solid line) smoothed to a lower resolution for sake of clarity, and combined with a previous low resolution spectrum¹⁷ of the full wavelength range $0.8 - 2.4\mu\text{m}$. At the quasar's redshift our data cover the wavelength range $1200 < \lambda_{rest} < 3300\text{\AA}$ in the rest frame of the emitted radiation. The observed spectrum is much bluer than LoBAL quasars observed at $z < 4$, whose average spectrum is shown with the dashed line¹³. In particular, SDSS1048+46 is bluer than *any* known LoBAL quasar¹³ at $z < 4$. Since the red shape of LoBAL quasars at $z < 4$ is ascribed to dust reddening, the much bluer slope of SDSS1048 already indicates a large variation of dust extinction and reddening from $z < 4$ to $z \approx 6$.

The continuum at $\lambda_{rest} > 1700\text{\AA}$ can

be fitted with a non-BAL (unreddened) quasar template with a slope $\alpha = -2.1$ ($F_\lambda \propto \lambda^\alpha$), which is shown with a dotted line in Fig.1. Such a blue slope is consistent with the intrinsic slope of -2.01 inferred by Reichard et al. (2003)¹³ for BAL quasars. The observed spectrum deviates significantly from the non-BAL unreddened template only at $\lambda_{rest} < 1700\text{\AA}$. While such a deviation was initially ascribed to a severe blend of the CIV and SiIV troughs in the low resolution spectrum, the new medium resolution spectrum (whose unsmoothed and enlarged version is shown in Fig. 1b) clearly shows that this is not the case. The continuum outside the troughs is indeed redder than expected by the extrapolation of the longer wavelength spectrum through the unreddened quasar template (dotted line). If such reddening at short wavelengths is due to dust, then the extinction curve must be quite unusual: relatively flat at $\lambda > 1700\text{\AA}$ and steeply rising at shorter wavelengths. We can quantitatively derive the extinction curve by using the equation $A_\lambda = -2.5 \log(F_{obs}/F_{intr})$, where F_{obs} is the observed spectrum and F_{intr} is the intrinsic spectrum. We avoided spectral regions contaminated by emission/absorption features by interpolating the continuum from the nearby regions. The blend of FeII lines²⁶ makes more uncertain the description of the continuum in the spectral region between 2300\AA and 3050\AA ; however, the latter spectral region is not critical within the context of this paper, since the most important aspect is that the extinction curve must be rather flat in the region between 1700\AA and 3300\AA , and increase rapidly at $\lambda_{rest} < 1700\text{\AA}$. For the intrinsic spectrum we used the non-BAL template obtained by the SLOAN survey¹³ (this choice is appropriate since non-BAL quasars at $z \sim 6$ have spectra similar to those at $z < 4$)¹⁷, with slopes ranging from $\alpha = -2.1$ (the reddest slope compatible with our observed

spectrum at $\lambda_{rest} > 1700\text{\AA}$) to $\alpha = -2.5$ (only 1% of quasars have slopes bluer than this value¹³). The resulting extinction curve is shown in Fig. 2 (thick solid line and shaded region). As expected, the extinction curve inferred for this quasar at $z = 6.2$ is quite different with respect to the SMC curve which applies to quasars at $z < 4$. The dot-dashed line in Fig. 1b indicates the non-BAL template absorbed with the extinction curve inferred by us in Fig. 2, which nicely matches the observed spectrum (except for the emission and absorption lines, whose intensity and shape depend on the physics of the ionized gas). The extinction $A_{3000\text{\AA}}$ required to match the observed spectrum is in the range 0.4–0.8 mag.

The extinction curve inferred from the most distant LoBAL can also reproduce the shape of the second most distant BAL SDSS1044-01, a High Ionization BAL (HiBAL)¹⁷ at $z = 5.78$. The latter quasar presents much lower reddening than SDSS1048-46 and therefore cannot be used to provide tight constraints on the extinction curve. Nonetheless, similarly to SDSS1048-46, it is characterized a rather blue continuum at $\lambda_{rest} > 1700\text{\AA}$ and a reddening at $\lambda_{rest} < 1700\text{\AA}$, which can be nicely fitted by using the same extinction curve derived above and shown in Fig. 2.

In order to interpret the observations, we have computed the SN dust extinction curve by using the model proposed by Todini & Ferrara (2001)⁶ which describes dust formation in the ejecta of Type-II SNe as a function of the progenitor mass and metallicity. In spite of the uncertainties, the model has been successfully applied to interpret the observed properties of SN 1987A⁶ and of the young, metal-poor dwarf galaxy SBS 0335-052²⁰. A grid of SN models has been considered, with different initial stellar progenitor masses ($12 M_{\odot} \leq M \leq 40 M_{\odot}$) and metallicities ($0 \leq Z/Z_{\odot} \leq 1$)²¹. The resulting SN dust grains are made

of silicates (Mg_2SiO_4 and MgSiO_3), amorphous carbon (AC), magnetite (Fe_3O_4) and corundum (Al_2O_3). The typical grain sizes range between 5 \AA to 0.1 μm , with smaller grains being predominantly composed of silicates and magnetite (sizes \approx 5–15 \AA) and larger ones by amorphous carbon (sizes \approx 100 – 200 \AA). The predicted grain properties for different Type-II SNe have then been averaged over the stellar Initial Mass Function (IMF). We adopted a Salpeter IMF, but even higher-mass weighted Larson-like IMFs²² do not change significantly the results ($\lesssim 2\%$ in the extinction curve).

The SN dust extinction properties have been derived using the standard Mie theory for spherical grains. Grains made of AC are the main contributors to extinction. We used the optical properties for AC produced in an inert atmosphere ($ACAR$ ²³), which is appropriate for the SN ejecta environment. Other important contributors to extinction were found to be Mg_2SiO_4 and Fe_3O_4 grains^{24,25}.

Fig. 2 shows the resulting extinction curves, which are in a much better agreement with the observations than the usual SMC curve. The extinction curves were obtained for various initial stellar metallicities. The best agreement is found for the $Z = 10^{-2} Z_{\odot}$ and $10^{-4} Z_{\odot}$ models, although the other models do not differ strongly and are still within the observational uncertainties. We also show the case of dust formed in the ejecta of a single $25 M_{\odot}$, $Z = 10^{-4} Z_{\odot}$ Type-II SN; the agreement for this case is excellent at most wavelengths. The plateau between 1700 \AA and 3000 \AA is due to a local minimum between two broad absorption features caused by AC grains, with the added flat contribution from Fe_3O_4 grains. Silicate grains contribute to the rise at shorter wavelengths.

We conclude that our analysis, combined with observations, provides the first direct evidence for dust produced in SN

ejecta, rather than in evolved stars, in an object at $z > 6$. In particular, we find that dust purely produced by Type-II SNe can explain very well the observed extinction curve. By implication, we conclude that much of the dust seen at high redshifts probably has the same origin. The properties of high redshift dust are therefore noticeably different from those found at later cosmic times: grains are typically smaller, due to their different formation history and to the short time available to subsequently accrete heavy atoms and coagulate with other grains.

Received 25 August 2018; Accepted —.

1. Hirashita, H., Ferrara, A. Effects of dust grains on early galaxy evolution *Mon. Not. R. Astron. Soc.* **337**, 921-937 (2002).
2. Schneider, R., Ferrara, A., Salvaterra, R., Omukai, K., & Bromm, V. Low-mass relics of early star formation. *Nature* **422**, 869-871 (2003).
3. Whittet, D. C. B. Dust in the galactic environment. Institute of Physics (IOP) Publishing, Bristol, 2003, Series in Astronomy & Astrophysics.
4. Bertoldi, F., Carilli, C. L., Cox, P., Fan, X., Strauss, M. A., Beelen, A., Omont, A., & Zylka, R. Dust emission from the most distant quasars. *Astron. Astrophys.* **406**, L55-L58 (2003).
5. Priddey, R. S., Isaak, K. G., McMahon, R. G., Robson, E. I., & Pearson, C. P. Quasars as probes of the submillimetre cosmos at $z > 5$ - I. Preliminary SCUBA photometry. *Mon. Not. R. Astron. Soc.* **344**, L74-L78 (2003).
6. Todini, P. & Ferrara, A. Dust formation in primordial Type II supernovae. *Mon. Not. R. Astron. Soc.* **325**, 726-736 (2001).
7. Nozawa, T., Kozasa, T., Umeda, H., Maeda, K. Nomoto, K. Dust in the Early Universe: Dust Formation in the Ejecta of Population III Supernovae. *Astrophys. J.* **598**, 785-803 (2003).
8. Schneider, R., Ferrara, A., Salvaterra, R., Dust Formation in Very Massive Primordial Supernovae. *Mon. Not. R. Astron. Soc.* accepted astro-ph/0307087 (2004).
9. Moseley, S. H., Dwek, E., Glaccum, W., Graham, J. R., Loewenstein, R. F. Far-infrared observations of thermal dust emission from supernova 1987A *Nature* **340**, 697-699 (1989).
10. Dunne, L., Eales, S., Ivison, R., Morgan, H., & Edmunds, M. Type II supernovae as a significant source of interstellar dust. *Nature* **424**, 285-287 (2003).
11. Morgan, H. L., Dunne, L., Eales, S. A., Ivison, R. J., & Edmunds, M. G. Cold Dust in Kepler's Supernova Remnant. *Astrophys. J.* **597**, L33-L36 (2003).
12. Richards, G. T., et al. Red and Reddened Quasars in the Sloan Digital Sky Survey. *Astron. J.* **126**, 1131-1147 (2003).
13. Reichard, T. A., et al. Continuum and Emission-Line Properties of Broad Absorption Line Quasars *Astron. J.* **126**, 2594-2607 (2003).
14. Hopkins, P., Strauss, M. A., Hall, P. B., et al. *Astrophys. J.*, in press. (2003, astro-ph/0406293)
15. Gaskell, C. M., Goosmann, R. W., Antonucci, R. R. J., Whysong, D. H., The Nuclear Reddening Curve for Active Galactic Nuclei and the Shape of the Infra-Red to X-Ray Spectral Energy Distribution *Astroph. J. submitted*, astro-ph/0309595 (2003)
16. Maiolino, R., Marconi, A., Salvati, M., Risaliti, G., Severgnini, P., Oliva, E., La Franca, F., & Vanzi, L. Dust in active nuclei. I. Evidence for “anomalous” properties. *Astron. Astrophys.* **365**, 28-36 (2001).
17. Maiolino, R., Oliva, E., Ghinassi, F., Pedani, M., Mannucci, F., Mujica, R. & Juarez, Y. Extreme gas properties in the most distant quasars. *Astron. Astrophys.* **420**, 889-897 (2004)
18. Baffa, C., et al. NICS: The TNG Near Infrared Camera Spectrometer. *Astron. Astrophys.* **378**, 722-728 (2001).

19. Maiolino, R., Juarez, Y., Mujica, R., Nagar, N. M., & Oliva, E. Early star formation traced by the highest redshift quasars. *Astrophys. J.* **596**, L155-L158 (2003). comments. This work was partially supported by the Italian Ministry of Research (MIUR) and by the National Institute for Astrophysics (INAF).

20. Hirashita, H., Hunt, L. K., Ferrara, A. Dust and hydrogen molecules in the extremely metal-poor dwarf galaxy SBS 0335-052. *Mon. Not. R. Astron. Soc.* **330**, L19-L23 (2002).

21. Woosley, S. E., & Weaver, T. A., The evolution and explosion of massive stars. II. Explosive hydrodynamics and nucleosynthesis. *Astrophys. J. Supp.* **101**, 181-235 (1995).

22. Early star formation and the evolution of the stellar initial mass function in galaxies. *Mon. Not. R. Astron. Soc.* **301**, 569-581 (1998).

23. Zubko, V. G., Mennella, V., Colangeli, L., Bussoletti, E. Optical constants of cosmic carbon analogue grains - I. Simulation of clustering by a modified continuous distribution of ellipsoids. *Mon. Not. R. Astron. Soc.* **282**, 1321-1329 (1996).

24. Scott, A., Duley, W. W. Ultraviolet and Infrared Refractive Indices of Amorphous Silicates *Astrophys. J. Supp.* **105**, 401-405 (1996).

25. Mukai, T. Cometary Dust and Interplanetary Particles in *Evolution of Interstellar Dust and Related Topics* Bonetti, A., Greenberg, J. M., Aiello, S. eds., (Elsevier Science Publishers, New York, 1989), 397-

26. Maiolino, R., Juarez, Y., Mujica, R., Nagar, N., Oliva, E. Early Star Formation Traced by the Highest-Redshift Quasars *Astroph. J.* **596**, L155-L158 (2003)

Correspondence and requests for materials should be addressed to Roberto Maiolino (e-mail: maiolino@arcetri.astro.it).

Acknowledgements All authors have contributed equally to this paper. We are grateful to J. Brucato for providing the optical constant of ACAR grains and we are grateful to M. Walmsley for useful

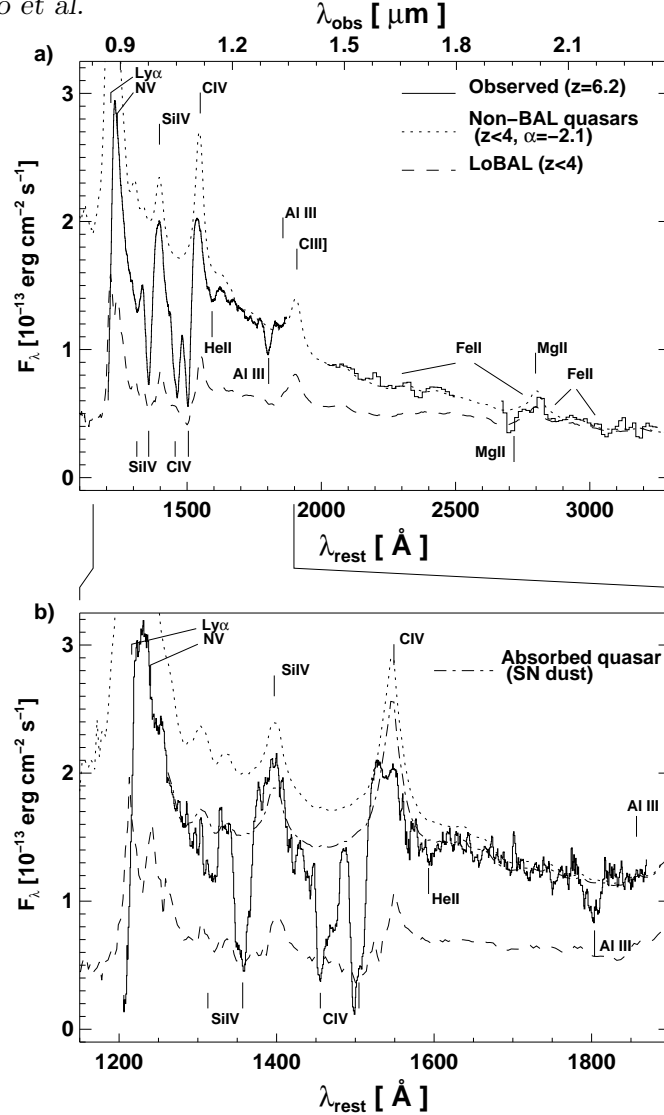


Figure 1. Spectrum of the quasar SDSS1048+46 at redshift 6.2, compared with quasar templates at lower redshift. a) The solid line shows the low resolution near-IR spectrum of the Low Ionization Broad Absorption Line (LoBAL) quasar SDSS1048+46. It is the composition of a previous low resolution $\lambda/\Delta\lambda = 75$ spectrum¹⁷ (shown only for $\lambda > 1.4\mu\text{m}$), and the new medium resolution $\lambda/\Delta\lambda = 350$ spectrum smoothed to a resolution of 75 for sake of clarity. Cross-calibration between the two spectra is ensured by matching the common parts. Upper labels identify the emission lines while lower labels identify the blueshifted absorption features. The presence of strong absorption from the high ionization species CIV $\lambda 1549$ and SiIV $\lambda 1397$, along with absorption by the low ionization species AlIII $\lambda 1857$ and MgII $\lambda 2798$ classifies this as a LoBAL quasar. The missing parts of the spectrum are due to the regions of bad atmospheric transmission. The dotted line is the average spectrum of (unreddened) non-BAL quasars at $z < 4$ with a slope $\alpha = -2.1$. The dashed line is the average spectrum of LoBAL quasars at $z < 4$. b) Same as above, but where the solid line shows only the (unsmoothed) medium resolution spectrum ($\lambda/\Delta\lambda = 350$) of SDSS1048+46. It is important to note the continuum level outside the troughs at $\lambda < 1700\text{\AA}$, which is well below the extrapolation of the continuum at longer wavelengths in the case of no dust reddening (dotted line). Both low and high resolution spectra allow the identification of the spectral regions for the continuum fitting (required to derive the extinction curve), and more specifically: 1275–1290 \AA , 1325–1340 \AA , 1417–1434 \AA , 1482–1489 \AA , 1577–1590 \AA , 1567–1677 \AA , 1708–1782 \AA , 1815–1845 \AA , 2015–2270 \AA , 3050–3255 \AA . The dot-dashed line in panel b) shows the effect of absorbing the non-BAL template with the extinction curve inferred by us and shown in Fig. 2 (thick solid line).

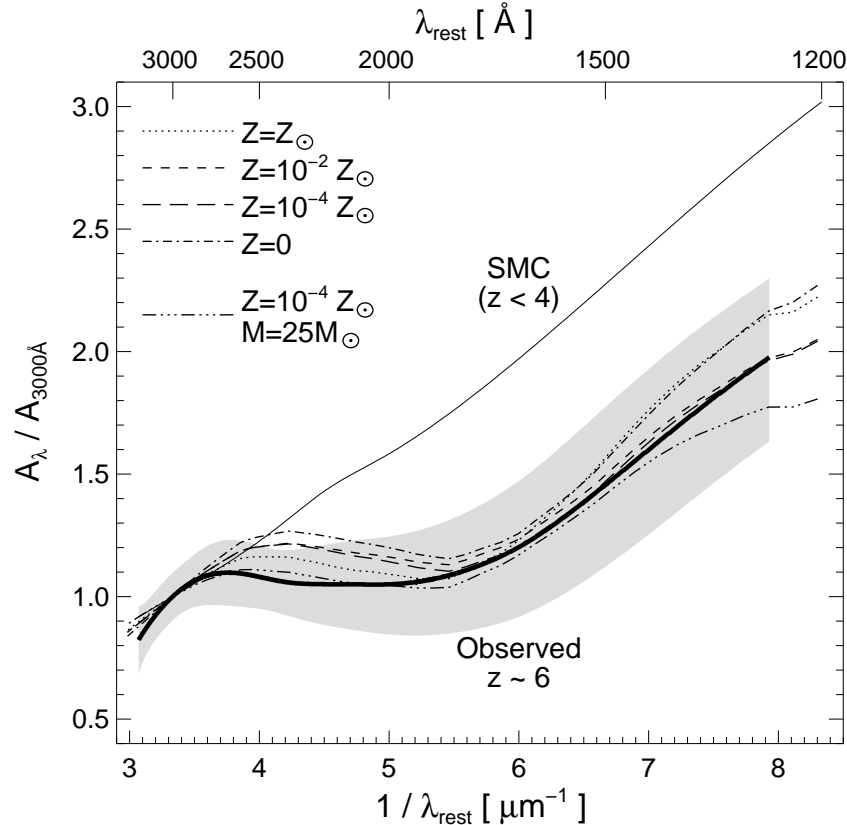


Figure 2. Extinction curve observed in the quasar SDSS1048+46 at $z = 6.2$ compared with the extinction curve observed in quasars at $z < 4$ and with the extinction curve expected from supernova (SN) dust. The thick solid line shows the extinction curve inferred for SDSS1048+46. The shaded area shows the associated uncertainty, which includes the range of intrinsic spectral slopes (this uncertainty dominates at short wavelengths, $\lambda < 1700\text{\AA}$), the uncertainty on the continuum interpolation (in particular around the FeII hump between 2300\AA and 3050\AA), and the noise in the spectrum. The thin solid line shows the Small Magellanic Cloud (SMC) extinction curve, which applies to quasars at $z < 4$ (including BAL quasars). The other lines indicate theoretical predictions for dust produced by SNe. More specifically: dot-dashed, long-dashed, short-dashed and dotted lines represent the extinction curves produced by SNe obtained assuming that stars form according to a Salpeter IMF and initial metallicities 0 , 10^{-4} , 10^{-2} , and $1 Z_{\odot}$, respectively. We also show the case of dust formed in the ejecta of a single $25 M_{\odot}$, $Z = 10^{-4} Z_{\odot}$ Type-II SN (triple-dot-dashed line).